



HAL
open science

ADVANCED STUDIES AND STATISTICAL TREATMENT FOR SODIUM-COOLED FAST REACTOR PIN FAILURES DURING UNPROTECTED TRANSIENT OVERPOWER ACCIDENT

Nathalie Marie, K Herbreteau, A Marrel, F Bertrand, A Bachrata

► **To cite this version:**

Nathalie Marie, K Herbreteau, A Marrel, F Bertrand, A Bachrata. ADVANCED STUDIES AND STATISTICAL TREATMENT FOR SODIUM-COOLED FAST REACTOR PIN FAILURES DURING UNPROTECTED TRANSIENT OVERPOWER ACCIDENT. Nuclear Science and Engineering, 2020, 10.1080/00295639.2020.1722542 . hal-03750679

HAL Id: hal-03750679

<https://hal.science/hal-03750679v1>

Submitted on 12 Aug 2022

HAL is a multi-disciplinary open access archive for the deposit and dissemination of scientific research documents, whether they are published or not. The documents may come from teaching and research institutions in France or abroad, or from public or private research centers.

L'archive ouverte pluridisciplinaire **HAL**, est destinée au dépôt et à la diffusion de documents scientifiques de niveau recherche, publiés ou non, émanant des établissements d'enseignement et de recherche français ou étrangers, des laboratoires publics ou privés.

ADVANCED STUDIES AND STATISTICAL TREATMENT FOR SODIUM-COOLED FAST REACTOR PIN FAILURES DURING UNPROTECTED TRANSIENT OVERPOWER ACCIDENT

N. Marie^{a*}, K. Herbreteau^a, A. Marrel^a, F. Bertrand^a, A. Bachrata^a

^a*CEA, DEN, DER, F-13108 Saint-Paul-lez-Durance, France*

*Corresponding author: nathalie.marie@cea.fr, Tel: +33 (0) 4 42 25 64 73, ORCID: 0000-0002-3756-7903

Abstract

Usually, simulation tools are validated on experimental data considering a Best Estimate simulation case and there is no quantification of this validation, which remains based on a rough expert judgment.

This paper presents an advanced validation treatment of the simulation tool OCARINa, devoted to Unprotected Transient OverPower (UTOP) accidents, on two CABRI tests, considering this time, a Best Estimate Plus Uncertainties (BEPU) approach. The output results of interest are both scalar physical data such as the time and location of the pin failure and associated molten mass and vector data such as temperature axial distribution or temperature evolution versus time. This approach is a first step in quantifying the degree of agreement between the calculation results and the experimental results. It is of great interest for the VV&UQ (Verification, Validation and Uncertainty Quantification) approach, which leads to the qualification of scientific calculation tools.

Within the framework of the Generation IV SFR R&D project in which the CEA is involved, OCARINa is a physical tool, relevant for performing pre-conceptual design studies, devoted to simulation of UTOP accidents on heterogeneous cores. Such accidents could not be simulated with mechanistic calculation tools such as SAS4A or SIMMER with their current capabilities; the thermomechanical models are not finalized in SIMMER tool and the SAS4A tool is only validated for homogeneous cores. The final objective aims at deriving the variability of the main results of interest to quantify the safety margins.

The final use of the OCARINa tool being to perform sensitivity studies on the various possible sodium fast nuclear pre-conceptual core designs, the validation of this tool is first discussed at the pin scale (where separate effect test measurements are available) based on statistical treatment. This enables to determine the lacks and uncertainties of this tool. The modeling is then extended from local pin behavior to global core behavior adding a point kinetic neutronic model. Final simulations of UTOP accidents caused by a uniform space reactivity ramp on an SFR (Sodium-cooled Fast Reactor) core are realized taking into account the specificities of the pins of the various assemblies. The orders of magnitude of mechanical energy released are derived.

Keywords: validation, CABRI, TOP, SFR

I. INTRODUCTION

A major innovation of the new Sodium-cooled Fast Reactor (SFR) French concept concerns the core, which is characterized by a very low (even negative) sodium void worth. In the framework of safety studies [1], the physical tool OCARINa, relevant for performing pre-conceptual design studies, is devoted to the Unprotected Transient OverPower (UTOP) accidents. It aims at deriving the variability of the main results of interest and to quantify the domain of safety margins related to the UTOP studies [2]. This is not achievable with current mechanistic tools requiring high CPU time and which are not completely adapted to the simulation of such accident on heterogeneous core design.

In the past, the methodology used in design studies and safety analysis of the severe accident of SFR was only based on one accidental scenario [3], reasonably bounding (expert judgment). This reference bounding scenario, which was an Unprotected Loss of Flow accident (ULOF), was simulated by mechanistic codes such as SAS4A [4] and SIMMER-III [5]. Currently the safety approach as regards mitigation of severe accident requires to simulate different possible accident scenarios classified into three main families: USAF (Unprotected Sub-Assembly Fault) [6], ULOF (Unprotected Loss Of Flow) [7], UTOP (Unprotected Transient OverPower [2]).

At that time, the OCARINa tool is limited to the simulation of a single pin during an UTOP. The key physical phenomena are described and modelled analytically in single pin geometry in accordance to the level of details required to catch all these decisive phenomena [2]. It involves a heat transfer and thermal-hydraulic solver chained with mechanical modeling in order to provide clad failure predictions and the evolution of the molten fuel mass and temperature in the fuel pin during the transient. The knowledge of these parameters is mandatory in order to engage the next steps of the transient modelling (fuel-coolant interaction, core power evolution and mechanical energy release). More specifically, the present model involves a one-dimensional radial transient conduction in the solid materials implicitly coupled with a one-dimensional transient mass and energy balance in the coolant. A dry-out model tackles the sodium voiding issue. The sodium flow is 1D and considered as unidirectional from the bottom (inlet) to the top (outlet). A mechanical post-processing using only analytical formulations is fulfilled at each time step [8]. The ultimate tensile stress of the clad, derived from this post-processing, is compared to a clad failure criterion expressed by the equivalent stress of the clad (also called von Mises strain).

This physical tool has been widely validated against separated test-cases using CESAR test loop facility results, CABRI test results and benchmarked with SIMMER-III calculations [5]. This work provides from an expert judgment “very good results” allowing to assert the validation of OCARINa. This previous work constitutes in a rough validation work, as usually done, by comparing each best-estimate simulation result with the corresponding experimental results (or benchmarked calculations).

In this paper, in the framework of a VV&UQ approach, a further assessment of the validation of the OCARINa tool is investigated. First, various types of results are available for each experimental CABRI test and it is worthwhile to value them further, through a multivariate validation. Secondly, we want to take into account the uncertainty on the input parameters of OCARINa tool as well as the experimental uncertainties. We want to consider the simulator in its entirety, i.e. both the OCARINa tool (and its model and numerical uncertainties) and its uncertain input parameters. Both elements constitute

the OCARINa simulator, as it will be used for prediction. The predicted output of the so-defined simulator is actually a probability distribution of the outputs, characterized by a range of possible values. Considering “the solver + input uncertainties” calls for a Best Estimate Plus Uncertainties (BEPU) approach, with a probabilistic framework. BEPU approach mainly relies on a probabilistic modeling of the model and input uncertainties and on their Monte Carlo sampling to propagate the uncertainty of the input parameters through the physical tool. In this validation framework with experimental results, the BEPU approach may also assess whether the simulated results are consistent with the possible range of experimental results. This will help to quantify the degree of agreement between the simulator and the experiments.

This BEPU validation study is realized on two very different CABRI experimental tests, namely CABRI-E7 and CABRI-E12, which are described in the next section. In section III, the statistical methodology is applied on the OCARINa tool: the obtained results are detailed, analyzed and put into perspective with the experimental results of CABRI-E7 and CABRI-E12. Having provided a preliminary quantified assessment of OCARINa on these experimental results and determined the uncertainties on the results of interest for the single pin case, the modeling is extended from local pin behavior to global core behavior. Simulations of UTOP accidents caused by a uniform space reactivity ramp on SFR core are given in section IV. A last section concludes the work and provides perspectives to continue the validation work for methodology establishment.

II. CABRI VALIDATION TESTS

The CABRI [9][10] facility is a 25 MW thermal nuclear reactor operated with light water reactor core devoted to power excursion studies. The In-pile test channel, containing only a single test pin in a sodium ascendant flow, is in the center of the core. The power transients are triggered with transient rods filled with gaseous Helium-3. Fast depressurization of these rods leads to a reactivity insertion in the core and a power increase up to 20 GW following a pulse-shape. For purpose of heat transfer and thermal-hydraulics models validation and clad mechanical failure model validation two very different CABRI tests, both involving clad failure, have been selected from the campaign CABRI-II: CABRI-E7 and CABRI-E12. Indeed, these tests present different types of fuel pin designs, burn-up and kinetics of the power excursion (see Table I) and completely different initial conditions, transient durations, and clad failure modes; thermally or mechanically induced.

II.A. CABRI-E7

The CABRI test E7 is the most energetic test of CABRI-II campaign, whereas CABRI-E12 is the less one. One of the special features of the E7 test is its high linear power during the steady state before the trigger of the power excursion (660 W.cm^{-1} compared to 450 W.cm^{-1} at the peak linear power location for a standard SFR pin). This very fast transient power excursion lasts less than 1 s. This test constitutes thus an extreme case where the fuel-melting margin is low even in steady-state regime before the power excursion transient (few hundred of degree). The pin failure is caused by the pressurization of the molten cavity in the pin, which presents a large radial extension (~85 % of the heated pin length located around the peak power location).

Transient	E7	E12
Type	TOP	Slow power ramp
$\frac{P_{max}}{P_0} (t_{Pmax})$	154 (450ms)	1,7 (86s)
Energy	injected at PPN: 1.67 (kJ/g)	ramp of ~0.9% P ₀ /s during 79s (P ₀ =474 W/cm)
Pin burn-up (at%)	4.6	12
Pin design	OPHELIE-6 (annular pellet)	VIGGEN-4 (solid pellet)

Table I. CABRI databases used for validation (TOP: Transient OverPower, P₀: initial power, P_{max}: maximum power, t_{Pmax} : time at P_{max} occurrence).

II.B. CABRI-E12

The CABRI-E12 test is the only slow power ramp test of the CABRI-II campaign having led to clad failure. The linear power at the peak power location of 474 W.cm⁻¹ in steady-state regime corresponds more to the operating domain of standard SFR pin. The transient is very slow and lasts 79s, standing for a control rod withdrawal accident. The clad rupture occurs at 76s as a result of the mechanical interaction between extended fuel pellet and the clad. Whereas all the other main key phenomena of these two transients are modeled in OCARINa (fuel phase change, solid thermal expansion and its influence on the mechanical stress, the various phenomena leading to clad failure; pressure of the molten cavity, the solid fuel and clad thermal expansion, contact pressure between fuel and clad, clad thermal melting...), it has been demonstrated in reference [2] that the very slow transients are at borderline of the validity domain of this physical tool. Indeed, the modeling of the radial heat exchange coefficient between the pellet and the clad (depending on the initial state (burn-up, fuel and clad temperature, power ...) but remaining constant during the transient in the OCARINa models [2]) is justified as long as the radial characteristic conduction time in the fuel (in the order of few seconds) is lower or in the order of magnitude of the transient duration. The CABRI-E12 test being a slow transient, the variation of this heat exchange coefficient has a non-negligible impact on the pin thermic, and thus on the thermomechanics and the clad failure. Nonetheless, this test has been selected owing to the low availability of data on the other CABRI tests with clad failure. In addition, it would allow a particular research study devoted to the consequences of the modeling bias of this coefficient on simulation results.

II.C. Set Of Experimental Data

Reports [9][10] provide experimental data of interest for these two CABRI tests.

The set of variables of interest and associated experimental uncertainties for this research study consists of:

1. Vector variables
 - Axial distribution of sodium temperature field in steady-state before the power excursion, $T_{NaPermanent}$ (K) – available in CABRI-E7 and two points are available in CABRI-12.

- Axial distribution of sodium temperature field at the clad rupture instant: $T_{\text{NaRupture}}$ (K) – only available in CABRI-E7.
2. Scalar variables
- Temperature difference along the heated channel in steady-state: dT_{NaP} (K). This value is 176.4 K in CABRI-E7 and 216K in CABRI-E12
 - Mass of molten fuel at the end of the transient: M_{liq} (kg). Only given in CABRI-E7: 0.204kg.
 - Axial location of the clad failure: z_{R} (m) which is 0.40 m from the bottom of the fissile zone in CABRI-E7 and 0.67m in CABRI-E12.
 - Instant of the clad failure occurrence: t_{R} (s) which is 0.467 s in CABRI-E7 and 76s in CABRI-E12.

The knowledge of the experimentally measurement uncertainties is also a crucial element for validation methodologies. Regrettably, it is a very tough job to obtain them with accuracy during the experimental campaign. Unfortunately, only pieces of information are collected on experimental uncertainties from experimental surveys, which permits to evaluate a rough order of magnitude of 5% around the measured values. As the distribution of this uncertainty has not been measured, we postulate, in a first approach, a truncated normal law distribution centered on experimental measure with a standard derivation of 5%.

III. ADVANCED METHODOLOGY VALIDATION

The OCARINa tool presents several uncertain inputs parameters and, in the framework of a BEPU approach, the objective of this paper is to propagate the uncertainty of the inputs and compare the OCARINa results with the available experimental data in order to validate the whole OCARINa simulator.

III.A. Uncertainty Input And Statistical Sampling

First of all, uncertainty inputs and their statistical sampling in the uncertainty variables space for uncertainty propagation should be defined. The uncertain variables are identified and characterized by probability density functions, in the framework of a probabilistic approach. A detailed analysis of the accidental scenarios leads to the identification of eight physically plausible independent random input variables for the UTOP test-case. The uncertainty sources are classified into two types: the initial test-case conditions and the models. Probability density functions (pdf) for the eight variables are identified and given in Table II. These pdf are either estimated from available experimental data from the literature or deduced from expert judgment. It means uniform law where there is no “most probable” value (all the values have the same probabilities) and truncated normal law otherwise.

Uncertain parameter and a review of the associated literature used to define pdf are described hereafter:

1. Variables linked to initial test-case conditions:
 - Fission product quantity trapped inside the pin in steady-state is a parameter which is involved in the calculation of the cavity pressure throughout fuel melting. As there is very few knowledge on this variable which depends on several data (such as the fuel burn-up, fuel temperature, power...), a uniform probability density law is assumed between two

realistic boundary values. The uppermost value of 10 mol has been derived from a simulation of the fuel behavior GERMINAL tool [11]. A realistic lower bound is taken to 1 mol which is an expert judgment as no data is available..

- The value of the coefficient of pellet/clad heat exchange. The SAS4A and SIMMER-III tools use around $5000 \text{ W.m}^{-2}.\text{K}^{-1}$ [4][5]. From GERMINAL simulations, it has been shown that, for fresh or low irradiated fuel, the pellet/clad heat exchange coefficient reaches $1.3 \cdot 10^4 \text{ W.m}^{-2}.\text{K}^{-1}$ and that it increases with the burn-up. Finally, it has been concluded that, this coefficient could be reasonably accurately fitted by a 10^α law with α following a uniform law between 3 and 5.
2. Variables linked to OCARINa models:

The retained uncertain variables are involved in thermal and mechanical models.

- Uncertainty on the value of the solid thermal conductivity determined on the basis of the Philipponeau correlation [12] and the associated probability density function issued from reference [13],
- Uncertainty on the value of the fuel liquid thermal conductivity at high temperature determined on the grounds of the only two values available in the literature [11]. Because of this lack of knowledge, a uniform probability density law is assumed between these two boundary values.
- Uncertainty on Nusselt number in the sodium flow. The truncated normal law is determined from the comparison of experimental data to the Lyon-Martinelli correlation [13].
- Uncertainty of the ultimate tensile stress of the clad issued on experimental correlations also used in GERMINAL [11]. These correlations give two values for this parameter (mean and maximum). The corresponding uncertain parameter follows a uniform law allowing a draw based on these two values.
- Uncertainty on the strain hardening modulus of the clad determined on the basis of experimental correlations issued from PHYSURAC [14].
- Uncertainty on the thermal conductivity of the shroud of CABRI test facility. This probability density function is issued from PHYSURAC [14].

The independence of these uncertain variables is an ordinary assumption.

Then, to propagate the uncertainties, a Monte Carlo-based sampling is considered, which yields a set of 1000 OCARINa simulations. This enables to investigate the domain of variation of the uncertain input parameters following their assumed probabilistic distributions. To generate this sample of inputs/outputs, we use here a space-filling design (SFD) of experiments, which provides a full coverage of the high-dimensional input space [15]. From the statistical sampling, the corresponding OCARINa outputs are computed. The realization of 1000 simulations required around 1 to 5 hours on 6 processors Intel Xeon E3-1230 v3. Note that, even if not presented here, convergence studies (with bootstrap approach [16]) have also been performed to ensure that was sufficient for achieving the convergence of statistical estimators.

Table II. Uncertain inputs parameters and their associated probabilistic model

Definition	Probability distribution	Distribution parameters			
		P1	P2	P3	P4
Initial conditions					
Fission product quantity trapped inside the pin [mol] (n_{PF})	Uniform	1	10		
Exponent α of the pellet/clad heat exchange coefficient [$W.m^{-2}.K^{-1}$] ($h_{jeu} = 10^\alpha$)	Uniform	3	5		
Modelling variables					
Uncertainty on the solid thermal conductivity (e_{kC})	Truncated normal	1	0.1	0.8	1.2
Fuel liquid thermal conductivity [$W.m^{-1}.K^{-1}$] (k_{Cl})	Uniform	2.52	6		
Nusselt number variation around the value given by the correlations of Lyon (1949) for sodium (e_{Nu})	Truncated normal	1	0.1	0.8	1.2
Uncertainty of the ultimate tensile stress of the clad (e_{Rm})	Uniform	0	1		
Uncertainty on the clad strain hardening modulus (e_K)	Truncated normal	1	0.1	0.8	1.2
Uncertainty on the shroud thermal conductivity (e_{kTH})	Truncated normal	1	0.1	0.8	1.2

With :

Probability distribution	Parameter P1	Parameter P2	Parameter P3	Parameter P4
Uniform	Minimal value	Maximal value		
Truncated normal	Mean	Standard deviation	Minimal value	Maximal value

Each of the 1000 OCARINa simulations consists in the establishment of the steady-state regime (steady-state temperature fields) followed by the power excursion transient corresponding to the simulated CABRI test. In order to reach the end of the calculation, one of the two following criteria must be fulfilled: either clad failure occurrence, or final transient time achievement.

III.B. Validation Results

The objective is to characterize the probabilistic distribution of the sample of OCARINa outputs.

III.B.1. Vector variables

The post-processing tool, used to visualize simultaneously several dependent vector data, is an adaptation of the Highest Density Region (HDR) boxplot [17][18]. This stands for the likelihood of vector OCARINa simulations with respect to the data measured in the experiments. From this, we can first assess the maximal level of the density region (noted α_{lik}) such as all the simulations are included in the finite range of

variations around the experimental data (or in a given confidence interval of the experimental data, confidence interval of level 95% for example). We expect from an accurate simulator a high value of α_{lik} (higher than 95% e.g.), which traduces that a high proportion of predictions are physically likely. The curve whose coefficients have the highest density is called the functional mode. Conversely, the curves whose coefficients have the lowest density are considered as outliers.

The distributions of the sodium temperature field along the heated pin, in nominal steady state ($T_{Na \text{ Permanent}}$) and at failure instant ($T_{Na \text{ Rupture}}$), for the 1000 simulations are plotted in figure 1 for CABRI-E7 tests: the dark and light grey areas are the density regions $R_{50\%}$ and $R_{90\%}$ respectively. The theoretical curve of highest density (estimated from the probabilistic modeling), which is called theoretical functional mode, is plotted in black solid line. The curve of highest density among the OCARINa simulations, which is called empirical functional mode, is plotted in black dotted line.

In steady-state results of CABRI E7 and E12, the empirical and theoretical mode are overlapped and the 90% density zone shows a deviation of 5 K for CABRI-E7 and 2 K for CABRI-E12. The very low discrepancy between the OCARINa predictions in permanent state is highlighted; all the predicted curves are overlapped. The uncertain parameters do not have any significant influence on the steady-state. This is physically justified by the fact that the temperature rise along the channel only depends on the linear power and the sodium flow rate (there are no heat leaks). The low discrepancy is only induced by the convergence criterion chosen to assess the steady state. For validation purpose, the measured experimental data, when available, with assumed uncertainties of 5% are also reported in this figure. For both test cases, all the simulations results are included in the error bar of the experimental results, which shows that OCARINa simulations are consistent with the experiments.

In the results, obtained at clad failure occurrence, of the axial sodium temperature distribution in CABRI-E7 and E12, the empirical and theoretical modes are overlapped. The 90% density zone shows a deviation of 30 K for CABRI-E7 and 6 K for CABRI-E12. The results discrepancy is more important in CABRI-E7 than in CABRI-E12. The available experimental results are included inside the 90% density zone; that quantifies the validation of OCARINa associated to the vector output variable. The lower variability in case of CABRI-E12 underlines the effect of the transient kinetics. The slow CABRI-E12 transient could be modeled by successive steady states (quasi steady state) where the transient terms have no influence (notably the thermal inertia of the pin [2]).

As the sodium-boiling margin when the clad fails (saturation temperature at $\sim 1170\text{K}$) is of 300K in CABRI-E7, the obtained deviation of 30K does not lead to overcome this saturation boundary. In CABRI-E12, the boiling margin is less (100K; the thermal equilibrium is reached and sodium heats-up owing to the slow transient). However, a dispersion of 6 K with a confidence level of 90% ensures the no boiling feature of the flow.

The margin to the sodium boiling has thus been quantified.

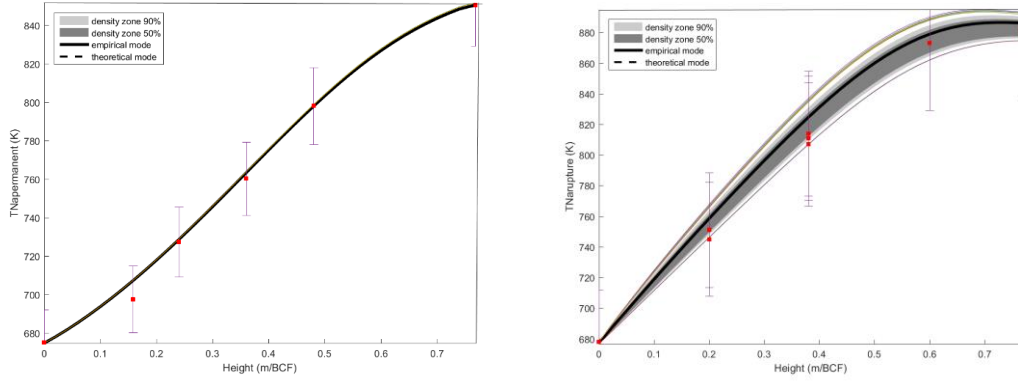


Figure 1. HDR-based visualizations of the axial distribution of T_{Na} permanent and T_{Na} Rupture for CABRI-E7 and experimental data (red dot) with uncertainty ranges

III.B.2. Scalar variables

In the framework of the advanced validation of OCARINa tool, we want to compare the OCARINa predictions to the CABRI experimental results. On one side, we have the numerical OCARINa tool with uncertain input parameter characterized by their pdf and, on the other side, we have experimental data tainted with measurement uncertainties. The objective is to assess if the OCARINa prediction is consistent with the experiments, whatever the value of the uncertain inputs.

The probability distributions of scalar outputs are given with an estimation obtained with a kernel density estimator^a (in solid black line). The CABRI experimental result is also added in red.

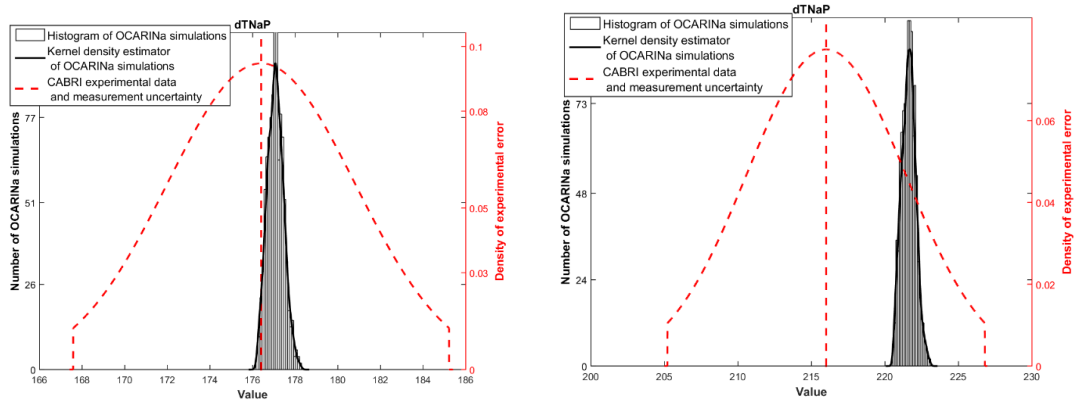


Figure 2. T_{NaP} - CABRI-E7 (left) and E-12 (right) – Distribution of the output parameters and CABRI experimental data in dotted red line

First, the sodium temperature difference along the heated channel at the beginning of the transient (dT_{NaP}) presents in figure 2, for CABRI-E7, a mode at 177K with a

^a kernel density estimation is a non-parametric way to estimate the probability density function of a random variable. Kernel density estimation is a fundamental data smoothing problem where inferences about the population are made, based on a finite data sample.

deviation of 2 K which covers the experimental value of 176.4 K. For CABRI-E12, the mode is 221.8K with a deviation of 2 K, and the experimental value of 216 K is outside the range of variation of OCARINa predictions. However, if we take into account the experimental uncertainties of 5%, the simulation mode, which is only 2.7% higher than the experimental data, remains inside the experimental error bar. The ranges of variation of simulations and experiments overlap.

When we now look at the molten fuel mass distribution Mliq (figure 3), it presents, for CABRI-E7, a mode at 0.208 kg (~30% of the total fuel pin mass) with a low deviation of 0.008kg that covers the experimental results of 0.204 kg. OCARINa predictions remain relatively consistent with experiments and its uncertainties, which validates OCARINa for Mliq.

For CABRI-E12, the distribution of OCARINa predictions is also very narrow with a mode at 0.04 kg and a deviation of 0.02 kg. The experimental value is not available but the simulation result, which corresponds to ~5% of the total fuel pin mass is less than the 10% stated in the literature [10].

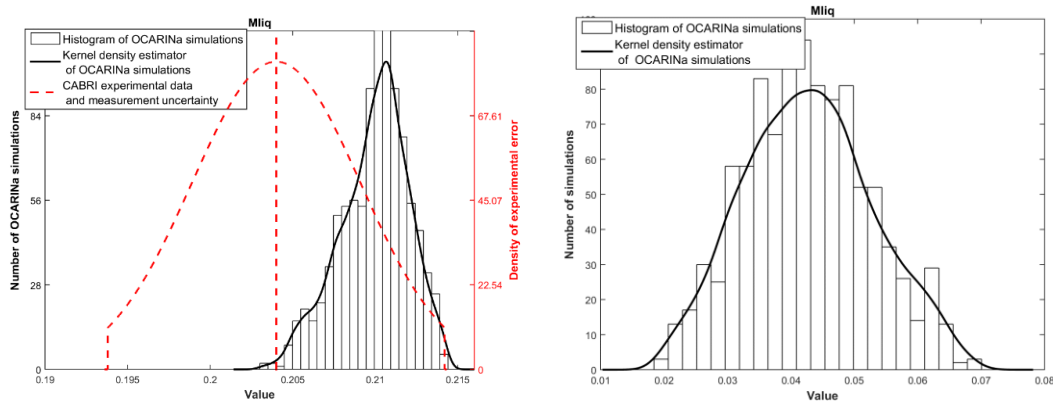


Figure 3. Mliq- CABRI-E7 (left) & E-12 (right) – Distribution of the output parameters and CABRI experimental data in dotted red line, when available

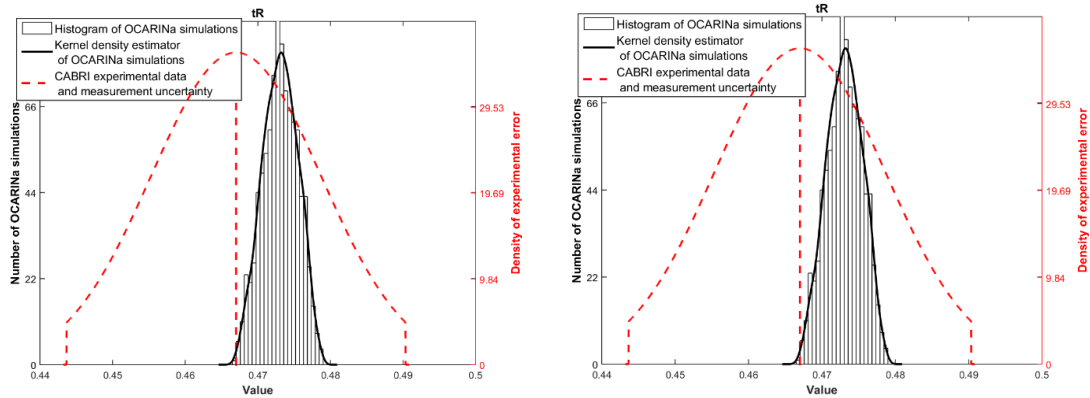


Figure 4. t_R - CABRI-E7 (left) & E-12 (right) – Distribution of the output parameters and CABRI experimental data in dotted red line

Regarding the clad failure (t_R), presented in figure 4, the simulations very well reproduce the instant of clad failure. In CABRI-E7, this distribution has a mode at 0.47 s with a low deviation of 0.01s covering, towards the low values, the experimental data of 0.47s. In CABRI-E12, the distribution has a mode at 75s with a deviation of 5 s. This time, the experimental value is within the higher values, at 76 s.

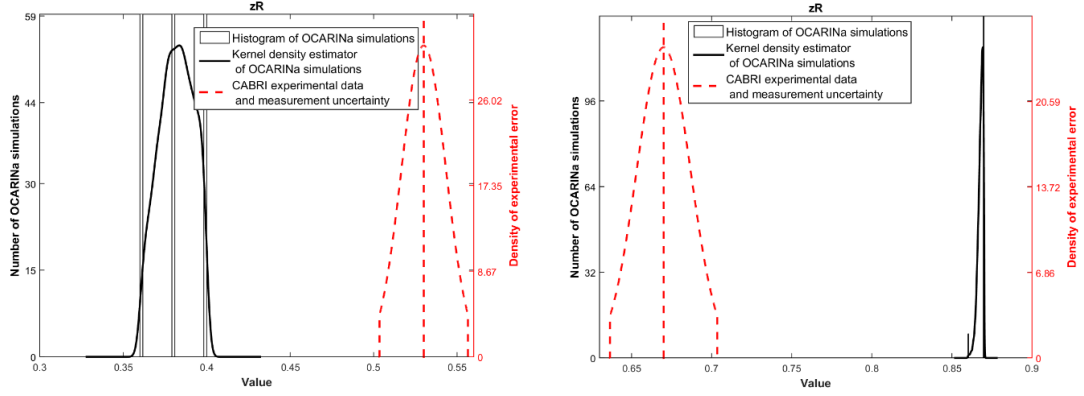


Figure 5. z_R - CABRI-E7 (left) & E-12 (right) – Distribution of the output parameters and CABRI experimental data in dotted red line

The elevation of the clad rupture (z_R) presents more discrete distributions owing to the discrete radial meshing; for CABRI E7, the failure occurs at a pin location covered by three consecutive meshes. This leads to three main results (see figure 5) among which 0.40 m is one of the modes. This value is the closest to the experimental result of 0.53 m, which is 20% higher than this mode. The ranges of variation of simulations and experiments do not overlap, which negates the validation. For CABRI-E12, almost all the simulations give the same clad failure elevation at 0.87 m whereas the experimental value is 0.67m. This value is 30% lower than the simulation results. This transient being slow, the clad temperature significantly rises and the mechanical properties are consequently deteriorated. The sodium temperature being, in a slow transient, maximum at the uppermost channel location, it is no surprising that the failure occurs at this location in OCARINa. In the reality, the pellet/gap heat transfer varies versus time, according to the pellet/clad gap closure, and this variation is not negligible during a slow transient. In this case, taking into account this variation, the heat flux released to the clad at the peak power elevation, where the clad thermal expansion is maximum, is the highest during the transient leading to more degraded mechanical properties and clad failure. This could explain the large discrepancy obtained between OCARINa and experimental results. A model to take into account the pellet/clad heat transfer evolution in OCARINa is under development to improve the prediction of the failure location.

To conclude on the validation of the OCARINa tool following the proposed validation methodology (based on a BEPU approach) on two very different test cases, it has been shown that for the vector and scalar data the ranges of variation of simulation results and experimental results overlap or are very consistent except for the failure localization, which is predicted at 20% and 30% respectively in CABRI-E7 and E12 (when experimental uncertainties are evaluated to 10-5%). This highlights a lack of models, especially for low transient, concerning the evolution of the pellet/clad heat exchange during the transient. Regarding the vector variables (temperature distribution field along the heated channel), all the BEPU curves lies in the 90% density zones, substantiating the validation of OCARINa. Then, the validation of this tool at the pin scale is encouraging but work remains to realistically simulate the failure localization.

The final use of the OCARINa tool is perform sensitivity studies on the various possible sodium fast nuclear pre-conceptual core designs. In this context its modeling is extended from local pin behavior to global core behavior and simulations of UTOP accidents caused by a uniform space reactivity ramp on SFR core are presented in the next section.

IV. PRELIMINARY CORE APPLICATION

Knowing the uncertainties linked to these data of interest on one single pin, the modeling is extended from local pin behavior to global core behavior considering the SFR core concept [19] which is an axial heterogeneous core of 1500 MWth on the contrary to more classical homogeneous cores used in former SFR.

The choice made in the representation of the core is a multi-1D modelling, with eleven hydraulic derivations gathering several assemblies (see figure 6) as it is usually done in CATHARE2 [20], MACARENa tool [21] or SAS4A [4]. Each of these assemblies is modeled as gathering 217 representative pins modeled as described in section I but with core features [19]. The global evolution of power in the core is given by a point-kinetics method, with 8 delayed neutrons precursor groups. The representation of the core allows taking into account specificities of each of the eleven groups of fuel assemblies: pressure drops, radial and axial power profiles, radial and axial profiles of the Doppler feedback effect and the number of fuel rods.

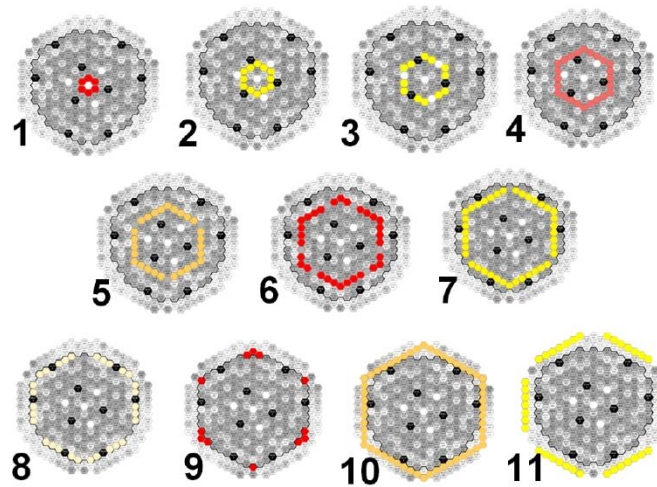


Figure 6. Schematization of the assemblies gather in the eleven derivations of OCARINA tool

Simulations of UTOP transients caused by a uniform space reactivity ramp on the SFR reactor core have been realized. An external ramp of reactivity insertion of $3\beta^b$ in one second has been considered corresponding to an accident of core support plate rupture. Sensitivity studies to the duration of this reactivity insertion have also been performed.

The reactivity variation, in such very fast UTOP transients, is predominantly governed by Doppler effect compared to thermal expansion effects which required much more time. The Doppler effect, which is associated to any change of temperature in the fuel, is given by a sum of the reactivity variations computed over each core mesh in the eleven representative SA. All the local feedback Doppler coefficients are derived from the neutronic tool ERANOS simulations [22]. This neutronic model is adequate because the simulation ends with the rupture of pins in the first assemblies, while the sodium voiding is still null or low, before their loss of geometry and thus spatial deformation of the power distribution.

^b $1\beta=370$ pcm in the core

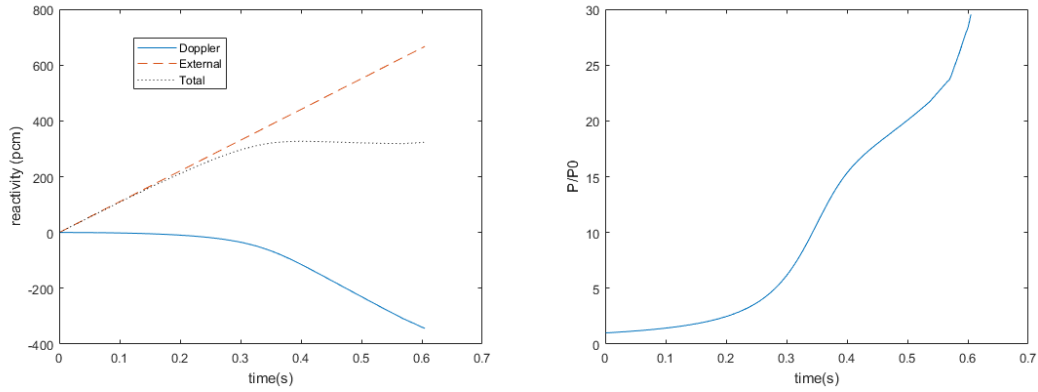


Figure 7. Evolutions of reactivity contributions and relative power in case of an external reactivity insertion of $3\$/s$

Considering various power transients, the variability of the main results of interest (time of the failure, fuel mass ejected inside the sodium...) have been investigated for each type of pins in the different assemblies. The main goal is to determine the first pins rupture and get the data to calculate the intensity of the consequent Fuel Coolant Interaction when molten fuel is ejected inside the sodium channel under the gas fission pressure motion and the associated reactivity effects resulting from these liquid fuel movements. This is an element of the evaluation of the global mechanical energy on the main vessel during an accident, evaluated by the analytical relation proposed by Hall [23]. It constitutes a safety criterion of around several hundreds of MJ depending on the reactor design [24].

Figure 7 presents the evolutions of the total reactivity and its various contribution as well as the relative power in case of an external reactivity insertion of $3\$/s$. The Doppler effect starts to have an influence when the relative power increase is sufficient to heat up significantly the fuel.

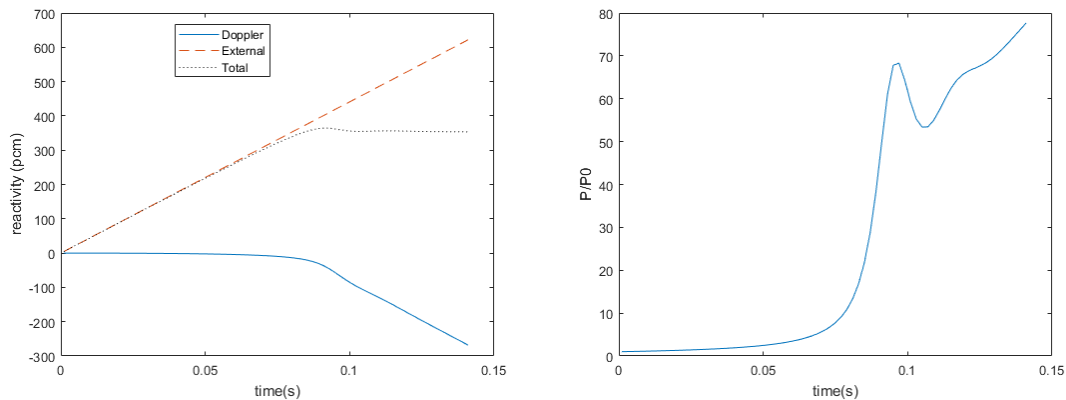


Figure 8. Evolutions of reactivity contributions and relative power in case of an external reactivity insertion of $3\$/0.25s$

Their results related to the two first failure pins event occurrence are presented in Table III. In case $3\$/0.25s$, prompt-criticality occurs at 0.84s (see figure 8 and no pins fail prior to this. In every cases, the pins of derivation 9, gathering 12 assembly, first break. For criticality ramp lower than 5s, the pins in derivation 3, gathering 12 other assemblies fail just after whereas, for slower criticality ramp, it is the pins in derivation 10 (gathering

54 assemblies) which secondly fail. The maximum mechanical energy obtained in every cases is very low, less than 1 MJ, far under the safety criterion.

Table III. Sensitivity study results to the duration of this reactivity insertion (derivation gathering assemblies are displayed in figure 6)

duration	0.25s	1s	5s	10s	60s
Prompt-criticality	0.084s	-	-	-	-
First pins failure occurrence	-	t=0.53s derivation 9	t=2.11s derivation 9	t=3.55s derivation 9	t=13.2s derivation 9
Second pins failure occurrence	-	t=0.57s derivation 3	t=2.26s derivation 3	t=3.85s derivation 10	t=14.8s derivation 10

V. CONCLUSIONS AND PROSPECTS

This paper deals with a new advanced statistical analysis applied to SFR pin design-oriented tool validation. As all the actual physical (mechanistic or designed or safety oriented) tool, the considered OCARINa tool has been widely validated against separated and integral experimental cases in the past. This validation commonly consists in the rough comparison between one experimental data (scalar or vector) to the corresponding best-estimate simulation result. This best-estimate simulation is performed with only the best-estimate value of each input and modelling parameters of the tool.

In the framework of VV&UQ methodology, an advanced validation is based on a Best Estimate Plus Uncertainties (BEPU) approach, taking into account the variability of most influential or varying input and model parameters. This validation allows a preliminary quantification of the degree of agreement between simulated and experimental results. This methodology has been applied on two very different CABRI tests: CABRI-E7 and CABRI-E12. They have permitted to conclude more accurately on the validation of the OCARINa tool on these two transients except for the prediction of the failure location. For that the distribution of the results of the OCARINa tool considering the uncertain input parameter (characterized by their pdf) are compared to the experimental data tainted with measurement uncertainties. Regarding the prediction of the failure location, models are under development to improve this prediction..

The final use of the OCARINa tool is to perform sensitivity studies on the various possible sodium fast nuclear pre-conceptual core designs. In this context, the physical modeling has been extended from local pin behavior to global core behavior considering the SFR core concept which is an axial heterogeneous core of 1500 MWth. Simulations of UTOP transients caused by a uniform space reactivity ramp on the SFR reactor core have been realized. An external ramp of reactivity insertion of 3\$ has been considered corresponding to an accident of core support plate rupture. Sensitivity studies to the duration of this reactivity insertion have been performed. Results on pins failure and associated mechanical energy releases have been derived, showing that the maximum mechanical energy obtained is very low, less than 1 MJ, far under the safety criterion.

In the future, regarding the statistical tool in support to the validation, an aggregated validation criterion will be developed to enable concluding on the global validation of a physical simulator tool regarding a coupled set of experimental results issued of one experimental test case, including as well scalar data as vector data. Moreover, the results of validation and sensitivity analysis depend on several prior

hypothesis concerning the probability distributions chosen for the uncertain inputs of the simulation tool and for experimental data. The latter only impacts the validation and can be taken into account by computing (and/or integrating) the validation for different assumed distributions. Concerning the prior distribution of the inputs of OCARINa which impact the distribution of the predicted outputs, it is more complicated, if we do not want make additional simulations of OCARINa. In the framework of sensitivity analysis, Meynaoui et al. [25] have recently proposed a solution to evaluate the impact of uncertainty on input distributions that they referred as “second-level uncertainties”. Their method relies on importance sampling technique, and keeps the same number of simulations. This method initially developed for sensitivity analysis, could be adapted for validation.

Regarding the OCARINa tool, physical model of evolution of the heat transfer between the fuel pellet and the gap will be added to realistically simulate the failure localization and validation process will be carried on.

REFERENCES:

- [1]. F. BERTRAND, et al., “Comparison of the behavior of two core designs for ASTRID in case of severe accidents”, *Nuclear Engineering and Design*, Vol. 297, pp 327-342 (2015).
- [2]. K. HERBRETEAU, et al., “Sodium-cooled fast reactor pin model for predicting pin failure during a power excursion”, *Nuclear Engineering and Design*, Vol. 335, pp 279-290 (2018).
- [3]. A.E. WALTAR, A.B. REYNOLDS, *Fast Breeder Reactors*. Pergamon. (1981)
- [4]. D. LEMASSON and F. BERTRAND, “Simulation with SAS-SFR of a ULOF transient on ASTRID- like core and analysis of molten clad relocation dynamics in heterogeneous subassemblies with SAS- SFR”, presented at ICAPP'14, Charlotte, USA (2014).
- [5]. S. KONDO, et al., “SIMMER-III: computer program for LMFR core disruptive accident analysis”, O-arai Engineering Center, Power Reactor and Nuclear Fuel Development Corporation (1996).
- [6]. N. MARIE, et al., “Physico-statistical approach to assess the core damage variability due to a Total Instantaneous Blockage of SFR fuel sub-assembly”, *Nuclear Engineering and Design*, Vol. 297, pp 343-353 (2016).
- [7]. J.B. DROIN, et al., “Physical tool for Unprotected Loss Of Flow transient simulations in a Sodium Fast Reactor”, *Annals of Nuclear Energy* 106 195–210, (2017).
- [8]. D. LAMKIN, “Analytical stress analysis solution for a simplified model of a reactor fuel element”, PhD thesis, University of Arizona (1974).
- [9]. M. HAESSLER et al., “The CABRI-II Programme—Overview on Results”, Proc. Int. Fast Reactor Safety Mtg., Snowbird, Utah, August 12–16, 1990, Vol. II, p. 209, American Nuclear Society (1990).
- [10]. I. SATO, et al., “Transient fuel pin behaviour and failure conditions in CABRI-2 in-pile tests”, In Proceedings of International Topical Meeting on Sodium Cooled Fast Reactor Safety, Obninsk, Russia, Oct 3–7 1994, Vol. 2, pp 134 (1994).
- [11]. J.C. MELIS, et al., GERMINAL – “A computer code for predicting fuel pin behavior”, *Journal of Nuclear Materials*, Vol. 188, pp 303-307 (1992).
- [12]. Y. PHILIPPONNEAU, “Thermal conductivity of (U,Pu)O_{2-x} mixed oxide fuel”, *Journal of Nuclear Materials*, Vol. 188, pp 194-197 (1992).
- [13]. A. MARREL, N. MARIE, M. DE LOZZO. “Advanced Surrogate model and sensitivity analysis methods for SFR accident assessment”, *Reliability Engineering and System Safety*, 138, 232–241, (2014)
- [14]. Le logiciel PHYSURAC, Objectifs, Description et Validation, CEA, rapport CEA-R-5200, http://www.iaea.org/inis/collection/NCLCollectionStore/_Public/15/001/15001924.pdf (1983).
- [15]. G. DAMBLIN, M. COUPLLET and B. IOOSS. “Numerical studies of space filling designs: Optimization of Latin hypercube samples and subprojection properties”, *Journal of Simulation*, Vol. 7, 276–289 (2015).
- [16]. B. EFRON et R.J. TIBSHIRANI, “An introduction to the Bootstrap”, CRC Press (1994).
- [17]. E. PARZEN. “On Estimation of a Probability Density Function and Mode”. *The Annals of Mathematical Statistics*, Vol. 33, pp 1065–1076 (1962).
- [18]. R.J. HYNDMAN, H.L. SHANG. “Rainbow plots, bagplots, and boxplots for functional data”. *Journal of Computational and Graphical Statistics*, Vol. 19, pp 29–45 (2010).

- [19]. P. SCIORA, et al., “Low void effect core design applied on 2400 MWth SFR reactor”, presented at ICAPP'15, Nice, France, 2011.
- [20]. N. ALPY, et al., “Phenomenological investigation of sodium boiling in a SFR core during a postulated ULOF transient with CATHARE 2 system code: a stabilized boiling case”, presented at NUTHOS-10, Okinawa, Japan, 2014.
- [21]. J.-B. DROIN, et al., “Uncertainty quantification on ULOF transients in a Sodium Fast Reactor”, submitted to Nuclear Engineering and Design
- [22]. G. RIMPAULT, et al., “The ERANOS code and data system for fast reactor neutronic analysis”, presented at PHYSOR 2002, Seoul, South Korea, October 7-10, 2002.
- [23]. A. N. HALL, “Outline of a new thermodynamic model of energetic fuel-coolant interactions”, *Nuclear Engineering and Design*, Vol. 109, pp 407-415 (1988).
- [24]. X. MANCHON, et al., “Modeling and Analysis of Molten Fuel Vaporization and Expansion for a Sodium Fast Reactor Severe Accident”, *Nuclear Engineering and Design* 322 (2017) 522-535.
- [25]. A. MEYNAOUI, A. MARREL, B. LAURENT, “New Statistical Methodology for Second Level Global Sensitivity Analysis,” *SIAM/ASA J. Uncertainty Quantif* (2019).